INTERNATIONAL JOURNAL OF OPTIMIZATION IN CIVIL ENGINEERING
Int. J. Optim. Civil Eng., 2020; 10(2):201-215

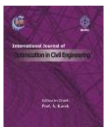

MODELING THE COMPRESSIVE STRENGTH OF CONCRETE MADE WITH EXPANDED PERLITE POWDER

D. Pourrostam[1], S. Y. Mousavi[2*, †], T. Bakhshpoori[3] and K. Shabrang[1]
[1]*Department of Civil Engineering, Rahman institute of higher education, Ramsar, Iran*
[2]*Department of Civil Engineering, Faculty of Engineering, Golestan University, Gorgan, Iran*
[3]*Faculty of Technology and Engineering, Department of Civil Engineering, East of Guilan, University of Guilan, Rudsar-Vajargah, Iran*

ABSTRACT

In recent years, soft computing and artificial intelligence techniques such as artificial neural network (ANN) and adaptive neuro-fuzzy inference system (ANFIS) have been effectively used in various civil engineering applications. This study aims to examine the potential of ANN and ANFIS for modeling the compressive strength of concrete containing expanded perlite powder (EPP). For doing this, a total of forty-five EPP incorporated concrete mixtures were produced and tested for compressive strength at different curing ages of 3, 7, 28, 42 and 90 days. Two different ANN models were developed and the suitable and stable ANN architecture for each model was considered by calculating various statistical parameters. For comparative purposes, two ANFIS models with different membership functions were also trained. According to the results, it can be concluded that the proposed ANN models relatively give a good degree of accuracy in predicting the compressive strength of concrete made with EPP, higher than that of observed from ANFIS models.

Keywords: Concrete, Expanded Perlite Powder, Compressive Strength, Artificial Neural Network, Adaptive Neuro-Fuzzy Inference System.

Received: 15 December 2019; Accepted: 12 March 2020

1. INTRODUCTION

Compressive strength is one of the fundamental properties of concrete which can also use as a qualitative measure for the other properties of hardened concrete [1]. Moreover, concrete in many structural applications is subjected to compression stresses and in this respect,

* 1Department of Civil Engineering, Faculty of Engineering, Golestan University, Gorgan
†E-mail address: Y.mousavi@gu.ac.ir (S. Y. Mousavi)

compressive strength of concrete is a required parameter in many design codes [1,2]. Generally, compressive strength of concrete depends on various factors such as degree of compaction, curing conditions, age, concrete mixture ingredients and proportions. Since the relationships between components of concrete and compressive strength are highly nonlinear, apart from multiple regression techniques, many researchers modeled the compressive strength of concrete by soft computing and artificial intelligence techniques like artificial neural networks (ANN), adaptive neuro-fuzzy inference system (ANFIS) and genetic programming. The use of these models can eliminate the need for extensive experimental investigation to better understanding the influence of mix ingredients on the compressive strength of concrete as a valuable property. Subsequently, this can save energy, cost, and time. In this regard, in a study by Kaveh and Khaleghi [3], ANNs are trained in order to predict the strength of concrete. Prediction of the compressive strength of self-compacted concrete by ANFIS models is illustrated by Vakhshouri and Nejadi [4]. Uysal and Tanyildizi [5] showed ANN can be an alternative approach for predicting the core compressive strength of self-compacting concrete mixtures with mineral additives. Kaveh et al. [6] suggested that tree based models perform remarkably well in predicting the mechanical and rheological properties of self-compacting concrete containing fly ash. Furthermore, some efforts have been made by researchers to predict the compressive strength of mortar or concrete containing metakaolin [7], silica fume [8], ground granulated blast furnace slag [9], rice husk ash [10] or nano-silica [11]. Nonetheless, there is still some concern regarding the lack of explicit formulation to effectively estimate the strength of concrete made with expanded perlite powder (EPP).

Perlite is a volcanic glass rock, located in many countries around the world such as Turkey, Greece, Hungary, etc. It is mainly composed of SiO_2 and Al_2O_3 and has little metal oxides such as sodium, potassium, iron, calcium and magnesium [12]. If natural raw perlite is subjected to a sudden temperature rise between 900 and 1200 °C, it expands up to 5-20 times of its original volume and transform into a cellular material, called “expanded perlite” [13]. Expanded perlite has particular physical properties such as low bulk density, low sound mission, high heat resistance and low thermal conductivity which led to effectively using expanded perlite in a various range of applications [14]. In the meantime, using perlite powder as an SCM in concrete is being a hot research topic with an interesting outlet. In this respect, Kotwica et al. [15] compared the pozzolanic activity of ground waste expanded perlite with commonly used commercial pozzolans and classified ground waste expanded perlite as pozzolanic material. Bektas et al. [16] reported that although both expanded and natural perlite powder have the potential to suppress the deleterious alkali–silica expansion, expanded perlite was more effective. Strength and permeability of concrete made with calcined perlite powder were investigated by Ramezanianpour et al. [17]. They found that although the compressive strength of concrete is insignificantly decreased when Portland cement was replaced by calcined perlite powder, the permeability is highly improved. Fodil and Mohamed [18] explored that 10% perlite powder in concrete resulted in an increase in the reduction of the corrosion rate in 5% of NaCl. Furthermore, the influence of waste expanded perlite on the chemical durability of mortars is investigated by Pichór et al. [19]. In this investigation, the potential of using ANN and ANFIS models for prediction of the compressive strength of EPP incorporated concrete at different curing ages is described. For this purpose, a wide range of experimental data at three water/cementitious materials ratios

(0.3-0.5), three cementitious materials content (350-450 kg/m^3) and five EPP replacement content (0-90 kg/m^3) were produced for building the models.

2. SOFT COMPUTING METHODS

2.1 Artificial neural network model

In the last few years, ANN has been applied in a great deal of civil engineering research domains such as shear strength of concrete [20], design of double layer grids [21] and structural optimization [22-24]. Neural network also has been used for prediction of moment-rotation characteristic for semi-rigid [25] and saddle-like connections [26], estimating the vulnerability of concrete moment resisting frame structures [27] and predicting the deflection of domes [28].

Inspiring from the biological neural systems of human brain, neural network has the ability to learn from experience, generalize from previous examples to new problems and make decisions [29]. Conceptually, ANN is a system of interconnected computational units, referred to as neurons. Each neuron receives the sum of the weighted inputs, adds a bias and generates the output by using an activation function. In a feed-forward neural network, the artificial neurons are arranged in layers that consist of an input layer, one or more hidden intermediate layers and an output layer [7]. Input information is received by the input layer and passes to the hidden layer(s) neurons, which then pass the information to the output layer [30]. In order to construct an effective ANN model, it first needs to be trained properly whereby the differences between actual and predicted values are minimized. This is done by adjusting the weights and biases through some training algorithm. This process is repeated until the network error reached to an appropriate value. In this study, back propagation neural network has been utilized due to its convenience to use [31] and widespread application in modeling the performance of concrete. New input-target values can be used to evaluate the efficiency of ANN model after the completion of the training process.

2.2 Adaptive neuro-fuzzy inference system

Neuro-fuzzy systems are formed from the connection of fuzzy systems with neural network in order to integrate the best features of both techniques. The architecture of ANFIS model with two inputs (x and y), two fuzzy IF–THEN rules based on Takagi and Sugeno's model and one output (f_i), which is presented in Fig. 1, can be described as follows:

$$\textit{Rule } 1\text{: } \textit{If } (x \textit{ is } A_1) \textit{ and } (y \textit{ is } B_1) \textit{ then } f_1 = p_1 x + q_1 y + r \tag{1}$$

$$\textit{Rule } 2\text{: } \textit{If } (x \textit{ is } A_2) \textit{ and } (y \textit{ is } B_2) \textit{ then } f_2 = p_2 x + q_2 y + r \tag{2}$$

where A_i and B_i are the linguistic labels, and p_i, q_i, and r_i are the consequent parameters that are determined during the training process. Regarding Fig. 1, the ANFIS has five layers. The functions of each layer are described subsequently:

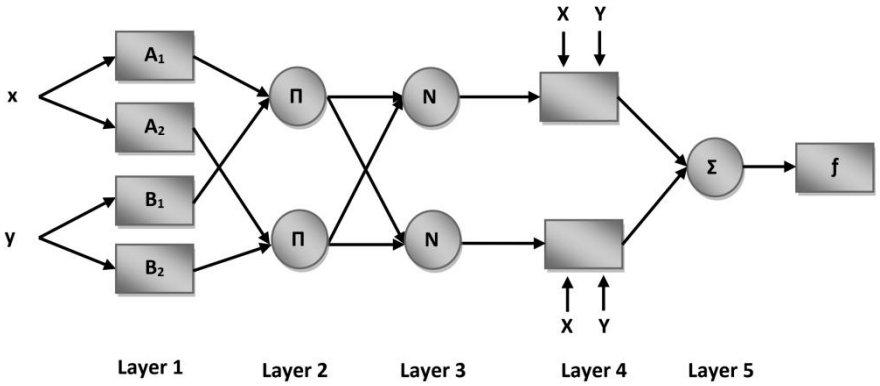

Figure 1. The architecture of ANFIS model [32].

Layer one: Every node in this layer is an adaptive node with a node function:

$$O_i^1 = \mu_{A_i}(x) \qquad \text{for } i = 1,2 \tag{3}$$

$$O_i^1 = \mu_{B_{i-2}}(y) \qquad \text{for } i = 3,4 \tag{4}$$

This layer tries to fuzzify the amount of the input variables [33]. The membership function, μ(x) or μ(y), can adopt any fuzzy membership function [34].

Layer two: Every node in layer two is a fixed node. The output is the product of all the incoming signals which can be presented as:

$$O_i^2 = w_i = \mu_{A_i}(x) \,.\mu_{B_i}(y) \qquad \text{for } i = 1,2 \tag{5}$$

The output of each node represents the so-called firing strength of a rule.

Layer three: Every node in this layer is a fixed node, representing the normalized firing strength of each rule. This is done by dividing firing strength of each rule by the sum of all the rules' firing strengths, as given by equation 6:

$$O_i^3 = \bar{w}_i = \frac{w_i}{w_1 + w_2}, \qquad i = 1,2 \tag{6}$$

Layer four: Every node in this layer is an adaptive node with node function:

$$O_i^4 = \bar{w}_i f_i = \bar{w}_i (p_i x + q_i y + r_i), \qquad i = 1,2 \tag{7}$$

where $\bar{w}_i$ is normalized firing strength from layer 3. Layer four is the defuzzification layer [35].

Layer five: Every node in this layer is a fixed node. The overall output by summation all

the inputs from the 4th layer is computed by equation 8.

$$O_i^5 = \sum_i \overline{w}_i f_i = \frac{\sum_i w_i f_i}{\sum_i w_i} \tag{8}$$

3. EXPERIMENTAL INVESTIGATION PLAN

In order to appraisal the effects of EPP on the compressive strength of concrete, 45 concrete mixtures were produced at three series namely "S1", "S2" and "S3". The details of the designed concrete mixtures were described in Tables 1 to 3. As can be seen in these tables, total cementitious materials contents for S1, S2 and S3 concrete groups were 350, 400 and 450 kg/m^3, respectively. Water-cementitious materials ratios (W/CM) were varied at 0.3, 0.4 and 0.5 in each concrete group and EPP was introduced at different replacement levels of 0%, 5%, 10%, 15% and 20%. These values were chosen based on the historical data and preliminary experimental investigation [9,36]. For all mixtures, sand/gravel ratio was kept constant at 0.83. At least 15 cubic specimens with side lengths of 100 mm were cast for each concrete batch and were compacted by using a vibrating table. The specimens were cured in water tank at 23 ± 2 °C. A total of 675 specimens were tested for compressive strength at different curing ages of 3, 7, 28, 42 and 90 days with a compression testing machine with a loading capacity of 2000 KN. It should be noted that the designations of concrete mixtures were accomplished according to the CM contents, EPP replacement ratio and W/CM ratio. For example, the "C35E5WCM0.4" designation was used for the concrete prepared with CM content of 350 kg/m^3, 5% EPP replacement ratio, and W/CM ratio of 0.4.

Table 1. Mixture proportions of S1 concrete group (TCM=350 kg/m^3).

	No.	Mix ID	W/CM	Cement	EPP		Water	sand	Gravel
				(kg/m³)	%	(kg/m³)	(kg/m³)	(kg/m³)	(kg/m³)
Total Cementitious Materials = 350 kg/m^3	1	C35E0WCM0.3	0.3	350	0	0	105	911.5	1093.9
	2	C35E5WCM0.3		332.5	5	17.5	105	908.9	1090.7
	3	C35E10WCM0.3		315	10	35	105	906.4	1087.6
	4	C35E15WCM0.3		297.5	15	52.5	105	903.8	1084.6
	5	C35E20WCM0.3		280	20	70	105	901.2	1081.5
	6	C35E0WCM0.4	0.4	350	0	0	140	869.7	1043.7
	7	C35E5WCM0.4		332.5	5	17.5	140	867.2	1040.6
	8	C35E10WCM0.4		315	10	35	140	864.6	1037.5
	9	C35E15WCM0.4		297.5	15	52.5	140	862.1	1034.5
	10	C35E20WCM0.4		280	20	70	140	859.5	1031.4
	11	C35E0WCM0.5	0.5	350	0	0	175	828	993.6
	12	C35E5WCM0.5		332.5	5	17.5	175	825.4	990.5
	13	C35E10WCM0.5		315	10	35	175	822.8	987.4
	14	C35E15WCM0.5		297.5	15	52.5	175	820.3	984.3
	15	C35E20WCM0.5		280	20	70	175	817.7	981.3

Table 2. Mixture proportions of S2 concrete group (TCM=400 kg/m^3).

	No.	Mix ID	W/CM	Cement	EPP		Water	sand	Gravel
				(kg/m^3)	%	(kg/m^3)	(kg/m^3)	(kg/m^3)	(kg/m^3)
Total Cementitious Materials = 400 kg/m^3	16	C40E0WCM0.3	0.3	400	0	0	120	874.7	1049.6
	17	C40E5WCM0.3		380	5	20	120	871.7	1046.1
	18	C40E10WCM0.3		360	10	40	120	868.8	1042.6
	19	C40E15WCM0.3		340	15	60	120	865.9	1039.1
	20	C40E20WCM0.3		320	20	80	120	862.9	1035.5
	21	C40E0WCM0.4	0.4	400	0	0	160	826.9	992.3
	22	C40E5WCM0.4		380	5	20	160	824	988.8
	23	C40E10WCM0.4		360	10	40	160	821.1	985.3
	24	C40E15WCM0.4		340	15	60	160	818.1	981.8
	25	C40E20WCM0.4		320	20	80	160	815.2	978.3
	26	C40E0WCM0.5	0.5	400	0	0	200	779.2	935
	27	C40E5WCM0.5		380	5	20	200	776.3	931.5
	28	C40E10WCM0.5		360	10	40	200	773.4	928
	29	C40E15WCM0.5		340	15	60	200	770.4	924.5
	30	C40E20WCM0.5		320	20	80	200	767.5	921

Table 3. Mixture proportions of S3 concrete group (TCM=450 kg/m^3).

	No.	Mix ID	W/CM	Cement	EPP		Water	sand	Gravel
				(kg/m^3)	%	(kg/m^3)	(kg/m^3)	(kg/m^3)	(kg/m^3)
Total Cementitious Materials = 450 kg/m^3	31	C45E0WCM0.3	0.3	450	0	0	135	837.8	1005.4
	32	C45E5WCM0.3		427.5	5	22.5	135	834.5	1001.4
	33	C45E10WCM0.3		405	10	45	135	831.2	997.5
	34	C45E15WCM0.3		382.5	15	67.5	135	827.9	993.5
	35	C45E20WCM0.3		360	20	90	135	824.6	989.6
	36	C45E0WCM0.4	0.4	450	0	0	180	784.1	940.9
	37	C45E5WCM0.4		427.5	5	22.5	180	780.8	937
	38	C45E10WCM0.4		405	10	45	180	777.5	933.1
	39	C45E15WCM0.4		382.5	15	67.5	180	774.2	929.1
	40	C45E20WCM0.4		360	20	90	180	771	925.1
	41	C45E0WCM0.5	0.5	450	0	0	225	730.4	876.5
	42	C45E5WCM0.5		427.5	5	22.5	225	727.1	872.6
	43	C45E10WCM0.5		405	10	45	225	723.8	868.6
	44	C45E15WCM0.5		382.5	15	67.5	225	720.5	864.7
	45	C45E20WCM0.5		360	20	90	225	717.3	860.7

The materials used in this study were type II Portland cement, EPP, natural aggregate, tap water and superplactizer. Portland cement was supplied from Hegmatan cement factory (Hamedan, Iran) with Blaine's specific surface area of 2910 cm^2/gr. Initial and final setting times of the Portland cement were 154 and 195 min, respectively. The chemical compositions of the Portland cement according to the producer data sheet were presented in

Table 4. Moreover, the used EPP was obtained from a local company and used in the production of concrete mixtures without any treatment. Chemical compositions of EPP were evaluated by X-ray fluorescence analysis and were described in Table 4. The coarse aggregate was crushed gravel with maximum aggregate size of 19 mm and well-graded natural river with specific gravity of 2.61 was used as fine aggregate. The super-plasticizer used in this study had a density of 1.1 g/cm^3.

Table 4. Chemical compositions of Portland cement and EPP.

Chemical composition (%)	PC	EPP
SiO_2	21.27	74.21
Al_2O_3	4.95	13.05
Fe_2O_3	4.03	1.09
CaO	62.95	0.87
MgO	1.55	0.34
SO_3	2.26	0.01
K_2O	0.65	5.38
Na_2O	0.49	2.42

4. DEVELOPMENT OF ANN PREDICTION MODELS

4.1 Data collection and preprocessing

A database for developing ANN models was experimentally produced (Tables 1-3) and the recorded data were randomly divided into three data sets.

The number of data used for the training process: 135 records (60 % of the total database).
The number of data used for the validating process: 45 records (20 % of the total database).
The number of data used for the testing process: 45 records (20 % of the total database).
Total number of data: 225 records.
In this study, all input and output data are normalized in the range of [0.1,0.9].

4.2 ANN modeling performance

Three indices including mean absolute percentage error (MAPE), root mean square error (RMSE) and absolute fraction of variance (R^2) were employed in order to examine the efficiency of the developed ANN models. These indices are defined as follow [37]:

Mean absolute percentage error (MAPE),

$$MAPE = \frac{1}{N}\sum_{i=1}^{N}\frac{\left|E_i - P_i\right|}{E_i}\times 100 \tag{9}$$

Root mean square error (RMSE)

$$RMSE = \sqrt{\frac{\sum_{i=1}^{N}(E_i - \mathrm{P}_i)^2}{N}} \tag{10}$$

Absolute fraction of variance (R^2)

$$R^2 = 1 - \frac{\sum_{i=1}^{N}(E_i - P_i)^2}{\sum_{i=1}^{N} P_i^2} \tag{11}$$

In these equations, E is experimental compressive strength results, P is predicted values and N is the total number of data points in each set of data. The smaller MAPE and RMSE values and the R^2 value close to one indicated the disparity between the network output and the experimental values is minimal.

4.2 ANN selection

As previously mentioned, the main objective of this research is to develop ANN and ANFIS models to predict the compressive strength of concrete made with EPP. For this purpose, two ANN models with different input variables were considered. They are C:EPP:W:T (Model A) and CM:EPP:W/CM:T (Model B) in which C, CM, EPP, W/CM, W and T stand for cement content, total cementitious materials content, expanded perlite powder content, water/cementitious materials ratio, water content and curing time, respectively. The compressive strength (CS) of concretes was as output parameter. The architecture of Models A and B was presented in Fig. 2.

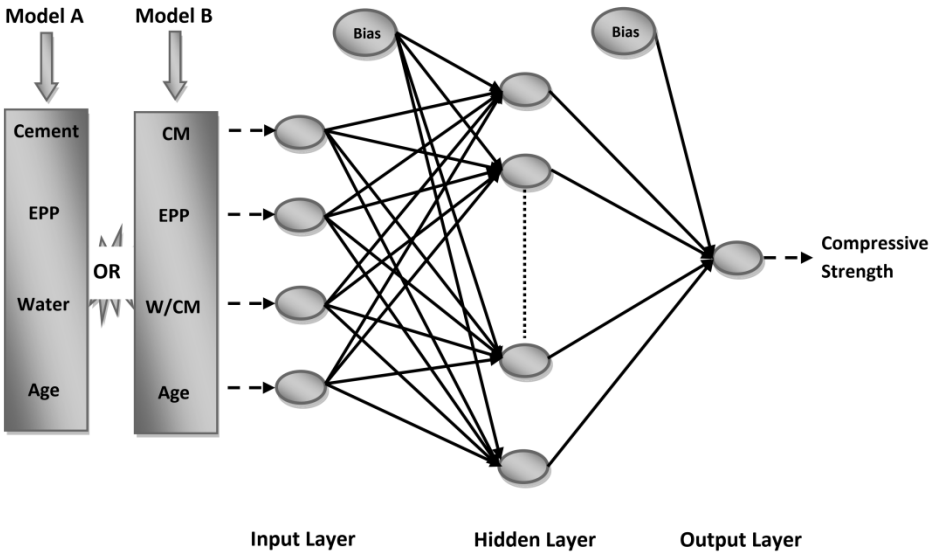

Figure 2. Architecture of Models A and B.

In this study, a program has been developed in MATLAB for derivation of the ANN models. For considering an appropriate architecture of ANN, the number of hidden neurons was varied and the suitable and stable ANN architecture was determined by calculating various statistical parameters (Eqs. 9-11) through the training process. Levenberg–Marquardt back propagation learning algorithm was employed as the training function. Moreover, the mean squared error was used as the performance function for training the ANNs. Sigmoid function was considered as an activation function and a linear function was used for the output layer.

Fig. 3 illustrated the MAPE, RMSE and R^2 values of the trained ANN models A and B with one hidden layer, respectively. It can be observed that in the case of model A (C:EPP:W:T), MAPE, RMSE and R^2 values are varied in the range of 1.876% to 6.1974%, 1.0576 to 3.6467 and 0.9956 to 0.9996, respectively. For model B (CM:EPP:W/CM:T), MAPE, RMSE and R^2 values were estimated between 2.5174%-6.8115%, 1.4574-3.6454 and 0.9957-0.9993, respectively. As presented in Fig. 3, for both models, as the number of hidden neurons increases, the values of MAPE and RMSE generally decreased and R^2 values approaching 1. Nonetheless, it is visible that there are no significant differences between the statistical parameters beyond a certain number of hidden neurons. In this respect, the appropriate number of neurons in the hidden layer of model A was chosen as 10, while the number of neurons in the hidden layer of model B is considered being as 12.

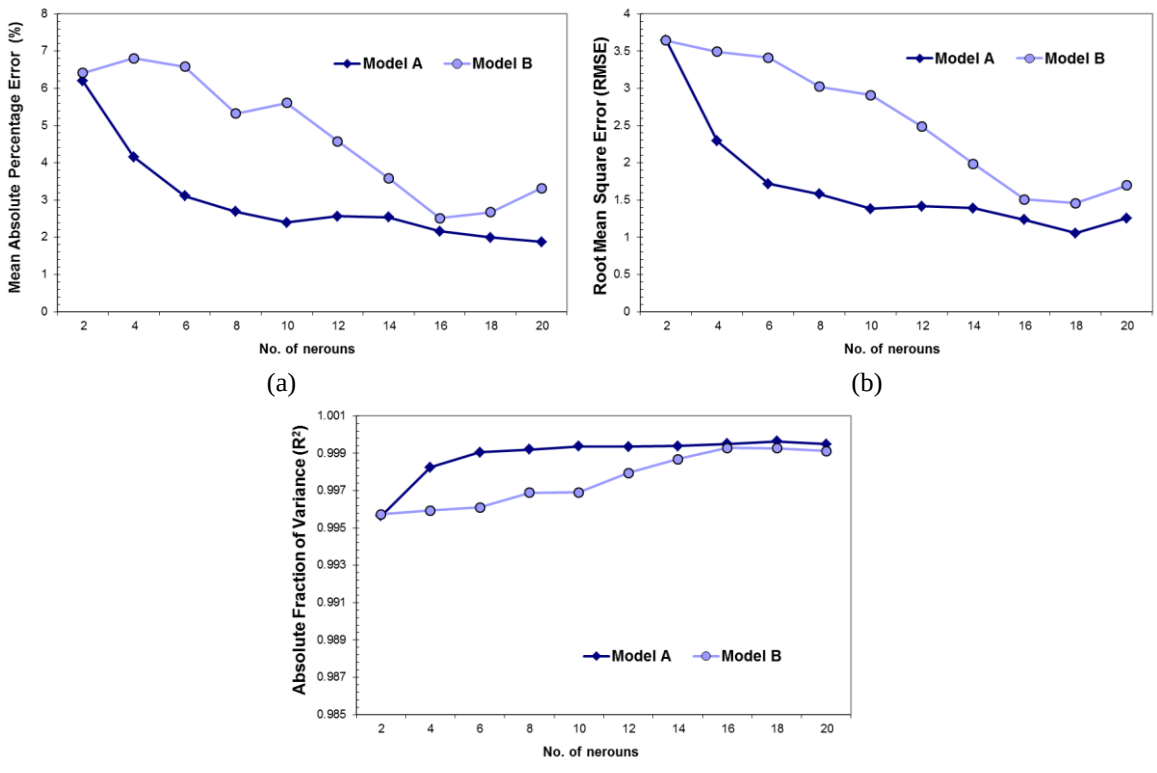

Figure 3. Statistical parameters of Models A & B throughout the training process.

4.2 ANN performance

After selecting the sufficient ANN architecture, predicted values are estimated for both models A and B. Fig. 4 (a) and (b) presented the scatter plots between measured and calculated results for the training, validating and testing data sets of models A and B, respectively. It can be observed that discrepancies from the line of equality are very small which demonstrated acceptable performance of the proposed ANN models in estimation of the compressive strength of concrete made with EPP. Moreover, results of ANN models performance levels investigated in terms of MAPE, RMSE and R^2 are tabulated in Table 5. Accordingly, MAPE, RMSE and R^2 for model A were 2.3942%, 1.3822 and 0.9994 for training data set, were 3.5462%, 2.1298 and 0.9985 for validating data set and were 3.8206%, 2.2869 and 0.9983 for testing data set. Regarding model B, for training, validating and testing data sets, the MAPE values were found out to be 4.5879%, 6.1009% and 6.5103%, RMSE values were 2.4844, 3.2180 and 3.3249 and R^2 were determined as 0.9979, 0.9968 and 0.9961, respectively. According to these results, MAPE and RMSE values are relatively low and R^2 is nearly close to unity. This is while it can be observed that model A exhibited somewhat better performance over model B.

Table 5. The performance of models A and B for training, validation and testing sets.

	Model A			Model B		
	Training	Validating	Testing	Training	Validating	Testing
MAPE	2.3942	3.5619	3.8593	4.5879	6.1009	6.5103
MSRT	1.3822	2.1298	2.2869	2.4844	3.2180	3.3249
R^2	0.9994	0.9985	0.9983	0.9979	0.9968	0.9961

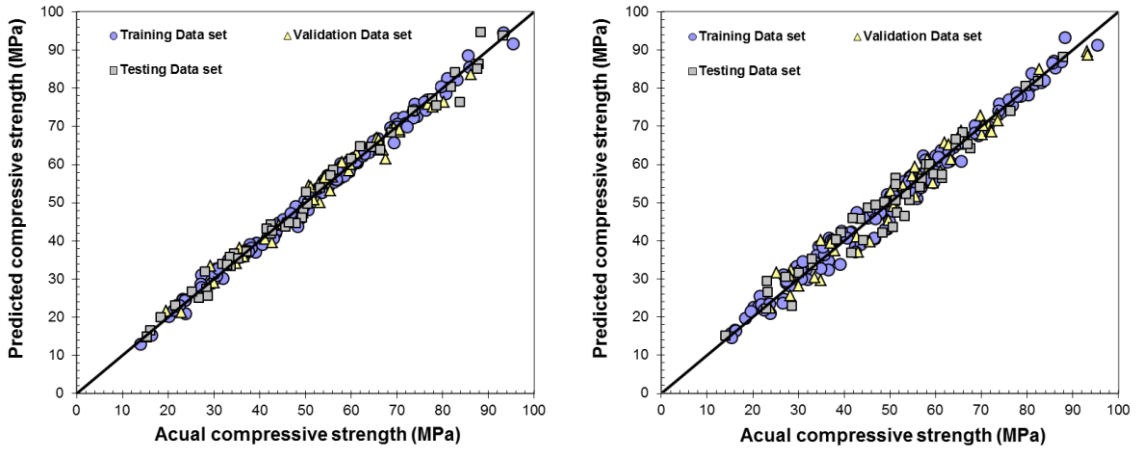

(a) (b)

Figure 4. Comparison of actual and predicted compressive strength from ANN related to (a) model A & (b) model B.

5. DEVELOPMENT OF ANFIS PREDECTION MODELS

In this study, the compressive strength of concrete made with EPP was also modeled by two different ANFIS models including C:EPP:W:T (Model A) and CM:EPP:W/CM:T (Model B). Among the total data (Tables 1-3), 135 records (60%) have been considered for training and the remaining records (40%) were used for testing the ANFIS models. Different membership functions were tried for each ANFIS model and the adequacy of the developed ANFIS models was examined by considering MAPE (Eq. 9), RMSE (Eq. 10) and R^2 (Eq. 11). Table 6 presents the utilized membership functions and Table 7 depicted the statistical parameters derived through the training and testing processes. It should be noted that the membership function parameters of ANFIS are adjusted by hybrid-learning method. A hybrid algorithm combines the gradient descent and the least squares method to solve the problems.

Table 6. The utilized membership functions.

	Type	Formula
trimf	triangular	$f(x;a,b,c)=\max\left(\min\left(\frac{x-a}{b-a},\frac{c-x}{c-b}\right),0\right)$
gbellmf	Generalized bell-shape	$f(x;a,b,c)=\frac{1}{1+\left\lvert\frac{x-c}{a}\right\rvert^{2b}}$
gaussmf	Gaussian	$f(x,\sigma,c)=e^{\frac{-(x-c)^2}{2\sigma^2}}$
dsigmf	Difference between two sigmoidal functions	$f(x;a,c)=\frac{1}{1+e^{-a(x-c)}}$

The results shown in Table 7 revealed that the statistical performance of ANFIS model A with "trimf" and model B with "gaussmf" is better than that with other membership functions. It can be concluded that the proposed ANFIS models have relatively enough accurately to model the compressive strength of EPP incorporated concrete. This can also be judged by observing the scatter plots between experimental results and predicted compressive strength by ANFIS models, presented in Fig. 5, where shows the points congregated about the diagonal line. It is concluded by comparing the obtained statistical parameters in Table 7 demonstrated that ANFIS prediction models A generally exhibits better prediction values than ANFIS Model B. Nonetheless, ANN prediction models have a better degree of coherency with experimentally evaluated compressive strength than the utilized ANFIS models.

Table 7. The performance of models A and B for training and testing data sets.

		Model A			Model B		
		MAPE	MSRT	R^2	MAPE	MSRT	R^2
trimf	Training	9.5e-7	0.0001	1	4.68e-06	0.0006	1
	Testing	6.3924	4.5461	0.9930	141.3620	13.1743	0.9360
gbellmf	Training	5.26e-06	0.0006	1	1.36e-05	0.0017	1
	Testing	9.9205	6.6545	0.9858	11.0311	8.6892	0.9739
gaussmf	Training	2.28e-06	0.0003	1	6.86e-06	0.0009	1
	Testing	7.3972	5.3760	0.9908	8.5276	6.8277	0.9843
gauss2mf	Training	4.69e-06	0.0004	1	8.85e-06	0.0011	1
	Testing	17.0760	8.6288	0.9756	18.2846	10.1472	0.9619
dsigmf	Training	6.38e-06	0.0007	1	1.47e-05	0.0013	1
	Testing	15.6217	8.3206	0.9772	591.8383	22.7198	0.7639

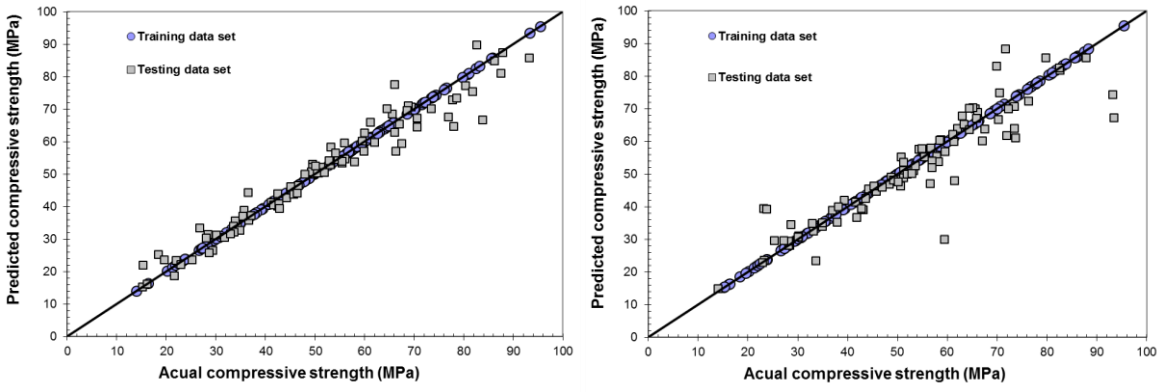

Figure 5. Comparison of actual and predicted compressive strength from ANFIS related to (a) model A & (b) model B.

6. CONCLUSION

In this study, compressive strength of concrete made with EPP was modeled by using ANN and ANFIS. To this aim, two ANN and two ANFS models were constructed where, cement content, EPP content, water content and curing age were considered as input variables for model A and the input variables for model B, were cementitious material content, EPP content, water/cementitious material ratio and curing age. By conducting extensive experimental investigations, 225 records were produced to derive the prediction model for the compressive strength of concrete made with EPP. According to the results:

1. After training different ANN prediction models A and B, there are no significant differences between the statistical parameters beyond a certain number of hidden neurons.

2. The MAPE, MSRT and R^2 values of ANN model A with 10 neurons in hidden layer were

of 3.8593%, 2.2869, and 0.9983 for the training data set, respectively. These value were 6.5103%, 3.3249, and 0.9961 for testing data of model B with 12 neurons in hidden layer, respectively.

3. Several membership functions were trained for each ANFIS model. "trimf" and "gaussmf" produces the best performance with the R^2 close to 1 and low MAPE and MSRE values for ANFIS model A and B, respectively.

4. Although, ANN and ANFIS models A and B can be helpful in prediction the compressive strength of concrete made with EPP, model A had pointed out a more reliable results.

5. Generally, results of this study demonstrated that ANN prediction models provided a better prediction values over ANFIS models.

REFERENCES

1. Shetty MS, Concrete technology. Theory and applications, Chand (S.) & Co Ltd ,India, 2006.
2. Golafshani EM, Behnood A, Arashpour M, Predicting the compressive strength of normal and High-Performance Concretes using ANN and ANFIS hybridized with Grey Wolf Optimizer, *Constr Build Mater* 2020; 232: 117-266.
3. Kaveh A, Khalegi A, Prediction of strength for concrete specimens using artificial neural networks, *Asian J Civil Eng* 2000; **1**(2): 1-12.
4. Vakhshouri B, Nejadi Sh, Prediction of compressive strength of self-compacting concrete by ANFIS models, *Neurocomputing* 2018; **280:** 13–22.
5. Uysal M, Tanyildizi H. Predicting the core compressive strength of self-compacting concrete (SCC) mixtures with mineral additives using artificial neural network, *Constr Build Mater* 2011; **25**(11): 4105-11.
6. Kaveh A, Bakhshpoori T, Hamze-Ziabari SM. M5'and Mars based prediction models for properties of self-compacting concrete containing fly ash, *Periodica Polytechnica Civil Eng* 2018; **62** (2): 281-94.
7. Sarıdemir M. Predicting the compressive strength of mortars containing metakaolin by artificial neural networks and fuzzy logic, *Adv Eng Soft* 2009; **40**: 920–7.
8. Özcan F, Atis CD, Karahan O, Uncuoglu E, Tanyildizi H. Comparison of artificial neural network and fuzzy logic models for prediction of long-term compressive strength of silica fume concrete, *Adv Eng Soft* 2009; **40**: 856–63.
9. Bilim C, Atis CD, Tanyildizi H, Karahan O. Predicting the compressive strength of ground granulated blast furnace slag concrete using artificial neural network, *Adv Eng Soft* 2009; **40**: 334–40.
10. Sarıdemir M. Genetic programming approach for prediction of compressive strength of concretes containing rice husk ash, *Constr Build Mater* 2010; 24: 1911–19.
11. Chithra S, Senthil Kumar SRR, Chinnaraju K, Ashmita FA. A comparative study on the compressive strength prediction models for High Performance Concrete containing nano silica and copper slag using regression analysis and Artificial Neural Networks, *Constr Build Mater* 2016; 114: 528–35.
12. Rashad AlM. A synopsis about perlite as building material – A best practice guide for Civil Engineer, *Constr Build Mater* 2016; **121**: 338–53.
13. Berge B. The ecology of building materials. Translated by Butters Chris and Henley Filip, Elsevier. 2009.

14. Naert KA, Wright LA, Thornton CP, Geology of the perlite deposits of the No Agua Peaks, Taos County, New Mexico: New Mexico Bureau of Mines and Mineral Resources, Open-file Report 162, 1980.
15. Kotwica Ł, Pichór W, Kapeluszna E, Różycka A. Utilization of waste expanded perlite as new effective supplementary cementitious material, *J Clean Prod* 2017; **140**: 1344-52.
16. Bektas F, Turanli L, Monteiro PJM. Use of perlite powder to suppress the alkali–silica reaction, *Cem Concr Res* 2005; **35**(10), 2014-17.
17. Ramezanianpour AA, Karein SMM, Vosoughi P, Pilvar A, Isapour S, Moodi F. Effects of calcined perlite powder as a SCM on the strength and permeability of concrete, *Constr Build Mater* 2014; **66**: 222-228.
18. Fodil D, Mohamed M. Compressive strength and corrosion evaluation of concretes containing pozzolana and perlite immersed in aggressive environments, *Constr Build Mater* 2018; **179**: 25-34.
19. Pichór W, Barna M, Kapeluszna E, Łagosz A, Kotwica Ł. The Influence of Waste Expanded Perlite on Chemical Durability of Mortars, *Sol St Phen* 2015; **227**: 194-8.
20. Amani J, Moeini R. Prediction of shear strength of reinforced concrete beams using adaptive neuro-fuzzy inference system and artificial neural network, *Scientia Iranica A* 2012; **19**(2): 242–8.
21. Kaveh A, Servati H. Design of double layer grids using back-propagation neural networks, *Comput Struct* 2001; **79**: 1561-8.
22. Iranmanesh A, Kaveh A. Structural optimization by gradient base neural networks, *Int J Numer Meth Eng* 1999; **46**: 297-311.
23. Kaveh A, Iranmanesh A. Comparative study of backpropagation and improved counterpropagation neural nets in structural analysis and optimization, *Int J Space Struct* 1998; 13; 177-85.
24. Kaveh A, Gholipour Y, Rahami H. Optimal design of transmission towers using genetic algorithm and neural networks, *Int J Space Struct* 2008; **23**(1): 1-19.
25. Kaveh A, Elmieh R, Servati H. Prediction of moment-rotation characteristic for semi-rigid connections using BP neural networks, *Asian J Civil Eng* 2001; **2**(2): 131-42.
26. Kaveh A, Fazel-Dehkordi D, Servati H. Prediction of moment-rotation characteristic for saddle-like connections using BP neural networks, *Asian J Civil Eng* 2001; **2**(1): 11-30.
27. Rofooei FR, Kaveh A, Masteri Farahani F. Estimating the vulnerability of concrete moment resisting frame structures using artificial neural networks, *Int J Operational Res* 2011; **1**(3): 433-448.
28. Kaveh A , Raiessi Dehkordi M. RBF and BP neural networks for the design of domes, *Int J Space Struct* 2003, 18(3): 181-94.
29. Chou J-Sh, Tsai Ch-F, Concrete compressive strength analysis using a combined classification and regression technique, *Automat Constr* 2012; **24**: 52–60.
30. Mukherjee A, Biswas SN, Artificial neural networks in prediction of mechanical behavior of concrete at high temperature, *Nuclear Eng Des* 1997; **178**: 1–11.
31. Yan F, Lin Zh, Wang X, Azarmi F, Sobolev K. Evaluation and prediction of bond strength of GFRP-bar reinforced concrete using artificial neural network optimized with genetic algorithm, *Compos Struct* 2016; **161**(1): 441–52.

32. Sobhani J, Ejtemaei M, Sadrmomtazi A, Mirgozar MA. Modeling flexural strength of EPS lightweight concrete using regression, neural network, and ANFIS, *Int J Optim Civil Eng* 2019; **9**(2): 313-29.
33. Dehnavi A, Nasiri Aghdam I, Pradhan B, Morshed Varzandeh MH, A new hybrid model using step-wise weight assessment ratio analysis (SWARA) technique and adaptive neuro-fuzzy inference system (ANFIS) for regional landslide hazard assessment in Iran. Catena 2015; **135**: 122–48.
34. Ceylan M, Arslan MH, Ceylan R, Kaltakci MY, Ozbay Y. A new application area of ANN and ANFIS: determination of earthquake load reduction factor of prefabricated industrial buildings, *Civil Eng Environ Syst* 2010; **27**(1): 53–69.
35. Jiang Zh, Zheng H, Mantri N, Qi Zh, Zhang X, Hou Zh, Chang J, Lu H, Liang Z. Prediction of relationship between surface area, temperature, storage time and ascorbic acid retention of fresh-cut pineapple using adaptive neuro-fuzzy inference system (ANFIS), *Postharvest Biol Tec* 2016; **113**: 1–7.
36. Tavakoli Abbandsaraei A. Effects of perlite powder on the properties of fiber-reinforcement high-strength concrete. MSc thesis, Golestan University, 2019.
37. Golafshani EM, Rahai A, Sebt MH, Akbarpour H, Prediction of bond strength of spliced steel bars in concrete using artificial neural network and fuzzy logic, *Constr Build Mater* 2012; **36**: 411–8.